



ACADEMIC
PRESS

Available online at www.sciencedirect.com

SCIENCE @ DIRECT®

Journal of Magnetic Resonance 161 (2003) 118–125

JMR
Journal of
Magnetic Resonance

www.elsevier.com/locate/jmr

Communication

Protein dynamics using frequency-dependent order parameters from analysis of NMR relaxation data

Djoudat Idiyatullin, Vladimir A. Daragan, and Kevin H. Mayo*

Department of Biochemistry, Molecular Biology & Biophysics, University of Minnesota Health Science Center, 321 Church Street, Minneapolis, MN 55455, USA

Received 5 June 2002; revised 8 October 2002

Abstract

A novel approach is described to analyze NMR relaxation data on proteins. This method introduces the frequency-dependent order parameter, $S^2(\omega)$, in order to estimate contributions to the generalized order parameter S^2 from different motional frequencies occurring on the picosecond to nanosecond time scales. $S^2(\omega)$ is defined as the sum of a specified set of weighting coefficients from the Lorentzian expansion of the spectral density function. ^{15}N NMR relaxation data (500, 600, and 800 MHz) on protein GB1 exemplify the method. Using this approach provides information on motional restrictions over specific frequency or time scale ranges and provides a normalized comparison of motional restrictions between proteins having different overall tumbling correlation times.

© 2003 Elsevier Science (USA). All rights reserved.

Keywords: GB1; ^{15}N relaxation; Molecular dynamics

1. Introduction and theory

The order parameter is a measure of the internal motional restriction of some vector, usually a N–H or C–H bond in a protein. It is perhaps the most important parameter currently used to describe intramolecular mobility. The generalized squared order parameter, S^2 , was defined by Lipari and Szabo [1,2] as

$$S^2 = \frac{4\pi}{5} \sum_{m=-2}^2 \langle Y_{2m}(\theta, \varphi) \rangle \langle Y_{2m}^*(\theta, \varphi) \rangle, \quad (1)$$

where Y_{2m} are spherical harmonics of the second order θ and φ and are polar angles for the motional vector within the molecular frame. Averaging is performed over all orientations of the motional vector. Considering only fast motions, like rotational fluctuations within a potential well (picosecond time scale), S^2 usually falls in the range of 0.9–1.0. For slower motions which occur with larger amplitudes like rotational conformational jumps (nanosecond time scale), S^2 is normally reduced

to 0.5–0.8, depending on amplitudes and correlations of these jumps [3,4].

Order parameters are usually derived from analysis of NMR relaxation data using some form of the spectral density function. The most popular approach was developed by Lipari and Szabo in 1982 [1,2], essentially assuming that the spectral density function can be described by two Lorentzians

$$J(\omega) = \frac{S^2\tau_o}{1 + (\omega\tau_o)^2} + \frac{(1 - S^2)\tau_i}{1 + (\omega\tau_i)^2}, \quad (2)$$

where $\tau_i = \tau_o\tau_i^R/(\tau_o + \tau_i^R)$ is the internal motional correlation time modified by the overall tumbling correlation time, τ_o , and τ_i^R is the actual internal motional correlation time. Although most often referred to as the ‘model free’ approach, this method is not truly ‘model-free’ because during derivation of Eq. (2) it was assumed that internal bond rotations within the molecule can be described by a single correlation time, τ_i . In fact, there are only two situations for which Eq. (2) is valid: isotropic overall tumbling with internal rotational jumps between n equivalent states or between two non-equivalent states. Even a simple model for rotational jumps between three non-equivalent states (e.g., trans-gauche

* Corresponding author. Fax: 1-612-624-5121.

E-mail address: mayox001@tc.umn.edu (K.H. Mayo).

transitions) requires the use of two internal motional correlation times. Clore et al. [5] found that in many cases, even with a limited amount of experimental data, at least three Lorentzians are required to describe the spectral density function, which in this case is expressed as

$$J(\omega) = \frac{S_f^2 S_s^2 \tau_o}{1 + (\omega \tau_o)^2} + \frac{S_f^2 (1 - S_s^2) \tau_s}{1 + (\omega \tau_s)^2} + \frac{(1 - S_f^2) \tau_f}{1 + (\omega \tau_f)^2}. \quad (3)$$

S_f , S_s , τ_f , and τ_s are order parameters and correlation times for fast and slow internal motions, respectively. Andrec et al. [6] later combined the use of Bayesian statistical methods and the Lipari–Szabo approach to estimate parameters from a multi-Lorentzian approximation of the spectral density function. Using a variation of the standard model free approach, LeMaster [7] analyzed NMR relaxation data using up to four internal motional correlation times, τ_i , with an expression for $J(\omega)$ like

$$J(\omega) = \frac{S^2 \tau_o}{1 + (\omega \tau_o)^2} + \sum_{i=1}^N \frac{c_i \tau_i}{1 + (\omega \tau_i)^2}, \quad (4)$$

where τ_i values are defined over a specific frequency range determined by Monte-Carlo minimization. Although it is impossible to determine individual correlation times and their weighting coefficients c_i from the limited number of experimental data for $N > 1$, LeMaster did demonstrate that the sum of c_i values can be determined accurately.

In proteins, there are numerous internal motional correlation times that could be derived to describe various rotational fluctuations and jumps within the backbone and side chains. Moreover, most protein molecules are non-spherical and overall tumbling of anisotropic molecules generally complicates analysis of NMR relaxation data. Therefore, it should not be surprising that Eqs. (2), (3), and even (4) are generally inadequate to analyze high quality NMR relaxation data collected at different frequencies, even though can allow many motional parameters to be determined. Nevertheless, due to the complexity of protein dynamics, some model assumptions must be made to simplify the analysis. One of the problems with using any of these ‘model free’ approaches is not knowing the number of Lorentzians required to fit $J(\omega)$. Having a good and relatively large set of NMR relaxation data allows one to use multiple Lorentzians to more accurately describe $J(\omega)$ [8]. In this regard, one should use the largest number of Lorentzians allowed by the number of experimental parameters. Another problem, rarely discussed but highly important, is the presence of relatively slow internal motions with correlation times τ_i^R larger than about $\tau_o/2$. In this case, corresponding τ_i values in Eqs. (2)–(4) will be nearly the same as the correlation time for overall tumbling, τ_o , and it would be nearly impossible to separate τ_i^R and τ_o ,

which leads to overestimated values of S^2 . This, in turn, also makes it difficult to compare order parameters from various sized proteins that have different overall tumbling correlation times. For one protein, internal motional correlation times may be near τ_o , and therefore inseparable from τ_o , whereas for another protein, they may be separable yielding a ‘less contaminated’ S^2 value.

To avoid such difficulties, it would be useful to have an order parameter that describes internal motional restrictions with correlation times defined over some specific frequency region. These frequency-dependent order parameters could be more easily compared among proteins of different size and shape, thereby providing deeper and more useful insight into protein dynamics in general. Here, we introduce the frequency-dependent order parameter, $S^2(\omega)$, to help visualize motional restrictions within various, yet specific, frequency ranges. This then allows for a better comparison of order parameters from different proteins. Here, we also provide the algorithm used to calculate $S^2(\omega)$. Use of this algorithm minimizes the normally deleterious effect from not knowing the actual number of modes involved in the motions of a particular vector, i.e., the precise number of Lorentzians needed to describe the spectral density function for that vector.

First of all, because it is reasonable to describe $J(\omega)$ as a sum of Lorentzians for any Markovian type of motion, the spectral density function generally can be written as

$$J(\omega) = \sum_{k=0}^m \frac{c_k \tau_k}{1 + \omega^2 \tau_k^2} + \sum_{k=m+1}^N \frac{c_k \tau_k}{1 + \omega^2 \tau_k^2}. \quad (5)$$

c_k and τ_k , $k = 0, 1, \dots, m$, are the weighting coefficients and correlation times describing overall molecular tumbling. Parameters c_k and τ_k for $k > m$ describe internal motions. For a spherical molecule, $m = 0$; whereas for symmetric top rotational diffusion, the number $m = 2$, and so on. The sums $\sum c_i$ are equal to

$$\begin{aligned} \sum_{k=0}^m c_k &= S^2, \\ \sum_{k=m+1}^N c_k &= 1 - S^2. \end{aligned} \quad (6)$$

N is the number of internal motional correlation times or motional modes.

The frequency-dependent order parameter, $S^2(\omega)$, is defined as the squared order parameter governing motions for any correlation time τ less than $1/\omega$. If the terms in Eq. (5) are sorted as $\tau_i > \tau_{i+1}$, one can write

$$S^2(\omega_k) = 1 - \sum_{i=k}^N c_i, \quad (7)$$

where $k > m$ is the motional mode number so that $1/\tau_i > \omega$ for any $i = k, k + 1, \dots, m$. The parameter

$S^2(\omega)$ has a simple physical meaning: it is the squared order parameter for all motions with motional frequencies greater than ω . At first glance, the method of LeMaster [7] appears similar to the $S^2(\omega)$ approach; however, the LeMaster method is quite different because it sums c_i values over the full frequency range of detectable internal motions and cannot be used to derive the frequency dependence of the order parameter as we are doing here.

According to Eqs. (5)–(7), $S^2(\omega)$ is related to the generalized order parameter, S^2 , by

$$S^2(\omega = 1/\tau_m) = S^2. \quad (8)$$

According to this definition, the limit $S^2(\infty) = 1$. In practice it is hard to determine the value of m . This problem is related to the general problem of separating overall tumbling and relatively slow internal motional correlation times, which will be considered in a separate paper. As shown below, it is convenient to calculate the function $S^2(\omega_k)$ for all k values as function of ω . In the case of an isotropic liquid, $S^2(\omega_0) = 0$. In the $S^2(\omega)$ plot, one observes a rather large inflection or drop in the function at low frequency. This drop corresponds to contributions from overall tumbling and relatively slow internal motions. Comparison of $S^2(\omega)$ plots for different proteins must be done for ω values that are far away from this drop. Fig. 1 exemplifies an $S^2(\omega)$ function, which has been calculated using three correlation times, τ_0 , τ_s , and τ_f . Note that the X-axis is given in units of

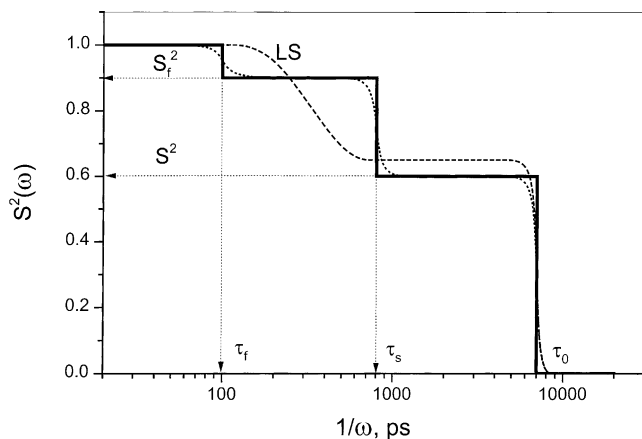


Fig. 1. Simulation of a $S^2(\omega)$ function for the motional model described by three correlation times: $\tau_0 = 8$ ns, $\tau_s = 800$ ps, and $\tau_f = 100$ ps. The solid line represents an ideal function of $S^2(\omega)$. Broader transitions (dotted lines) are normally observed due to experimental errors, insufficient data, and/or distributions of internal motional correlation times. The Lipari–Szabo approximation (two Lorentzians) is schematically shown by the dashed line and labeled with ‘LS’. The generalized order parameter, S^2 , can be read from the lower plateau, whereas the upper plateau indicates the order parameter for fast motions, S_f^2 defined by Clore et al. [5]. Correlation times for overall tumbling, τ_0 , slower nanosecond time scale internal motions, τ_s , and faster picosecond time scale internal motions, τ_f , are read from the transition points as indicated.

$1/\omega$ for easier readout of correlation time regimes. Steps (solid lines) are observed when $1/\omega$ is equal to its respective correlation time. The S^2 limit in $S^2(\omega)$ is observed for the correlation time range τ_s – τ_0 . In practice, factors like experimental error, insufficient data, and distributions of internal motional correlation times, tend to broaden these unrealistically sharp transitions as illustrated by the dotted line. If one uses a small number of Lorentzians to describe $S^2(\omega)$, i.e., the Lipari–Szabo approximation with two Lorentzians, the finer details disappear as schematically illustrated by the dashed line in Fig. 1.

To use this method, one needs to determine the coefficients c_i and correlation times τ_i , for $i = 0, 1, \dots, N$, with N being as large as possible for any given set of experimental data. With three relaxation parameters, e.g., T_1 , T_2 , and NOE, acquired at three magnetic field strengths, there are nine experimental parameters that can be used to determine up to nine theoretical parameters, i.e., five Lorentzians in Eq. (3) if one takes into account that $\sum c_i = 1$. Although it is practically impossible to obtain reliable values of c_i and τ_i for $N > 2$, linear combinations and other functions of c_i and τ_i over some frequency range are very stable and can be determined accurately as shown by LeMaster [7]; see also [8] and [9].

To estimate errors in determining $S^2(\omega)$ using relaxation data acquired at three magnetic fields, a simple Monte-Carlo procedure [6] was used as outlined in the following algorithm:

1. Randomly take five values of correlation times τ_i : $0 < \tau_i < t_1$. To cover a range of possible errors in the estimation, as well as the influence of rotational anisotropy, t_1 should be about 50–70% larger than the estimated overall correlation time τ_0 for a given protein molecule. To estimate τ_0 , one can use the empirical equation $\tau_0 = (9.18 \times 10^{-3}/T) \exp(2416/T) n_R^{0.93}$, where n_R is the number of residues, T is the temperature in K [4].
2. Use any minimization program to find appropriate values of c_i that best fit the experimental data, i.e. minimize the sum of nine terms $\chi^2 = (1/9) \sum (R_j - R_j^{\text{calc}})^2 / \sigma_j^2$, where R_j are experimental parameters; R_j^{calc} are calculated parameters, and σ_j are the experimental errors in determining R_j . If $\chi^2 < 1$ store the set of c_i and τ_i . Repeat steps 1 and 2 if $\chi^2 > 1$.
3. Repeat this process n times (usually $n = 100$ – 200) to obtain n sets of c_i and τ_i . For each k th set of c_i , calculate $S^2(\omega)_k$ from Eq. (7). The probability, P_k , of finding the k th set of c_i and τ_i as [6]

$$P_k = \prod_{j=1}^9 \frac{1}{\sqrt{2\pi\sigma_j^2}} \exp \left[-\frac{(R_j - R_{jk}^{\text{calc}})^2}{2\sigma_j^2} \right], \quad (9)$$

where R_{jk}^{calc} are calculated parameters for the k th set.

4. Use $5n$ weighted Lorentzians to describe $J(\omega)$. The average value of $S^2(\omega)$ and the standard deviation $\Delta(\omega)$ of $S^2(\omega)$ can be calculated as

$$\begin{aligned} S^2(\omega) &= \sum p_k S^2(\omega)_k, \\ \Delta^2(\omega) &= \sum p_k [S^2(\omega) - S^2(\omega)_k]^2, \end{aligned} \quad (10)$$

where $p_k = P_k / \sum P_k$.

This procedure allows one to obtain smooth the transitions as illustrated by dotted lines in Fig. 1. The appearance of non-sharp transitions between motional modes essentially results from experimental errors in the relaxation parameters and distributions of correlation times. For this reason, the symbol $S^2(\omega)$, rather than $S^2(\omega_k)$, will be used throughout the remainder of the text.

Fig. 2 illustrates model calculations of $S^2(\omega)$ using NMR relaxation parameters calculated by assuming that molecular motions are described by three Lorentzians with $\tau_0 = 6000$ ps, $\tau_1 = 1000$ ps, $\tau_2 = 10$ ps, $c_0 = 0.5$, $c_1 = 0.4$, and $c_2 = 0.1$. In order to appreciate differences in using different numbers of Lorentzians to fit relaxation data, both two- and five-Lorentzian approximations of $J(\omega)$ were used to calculate $S^2(\omega)$ as

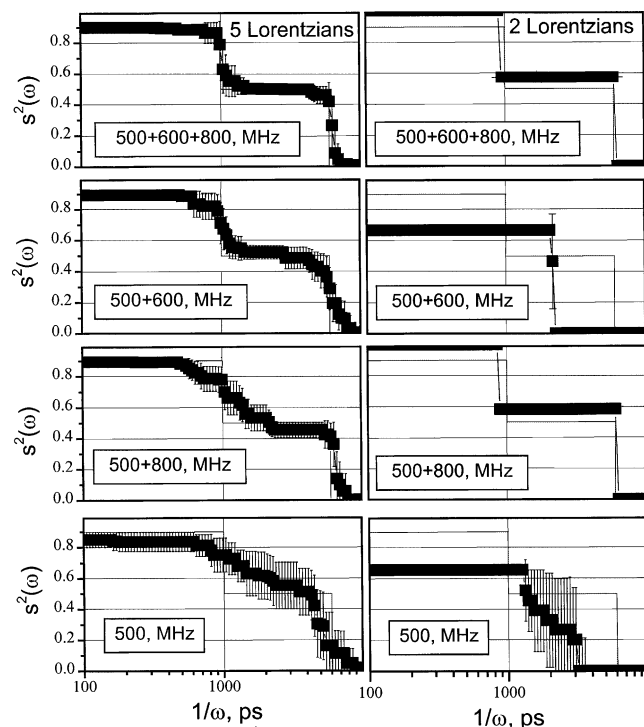


Fig. 2. Model calculations of $S^2(\omega)$ from relaxation data simulated for different NMR frequencies (500, 600, and 800 MHz ^1H spectrometer frequencies) as indicated in the figure. The simulation was performed by assuming that molecular motions were described by three Lorentzians with parameters: $\tau_0 = 6000$, $\tau_1 = 1000$ ps, $\tau_2 = 10$ ps, $c_0 = 0.5$, $c_1 = 0.4$, and $c_2 = 0.1$. Left and right panels represent simulations performed using five and two Lorentzian approximations, respectively. Error bars were computed as discussed in Section 1.

shown in the figure. Although using relaxation data acquired at three frequencies (500, 600, and 800 MHz) yields the best results, it is readily apparent that use of the five-Lorentzian approximation with data acquired at only two frequencies (500 and 600 MHz) provides a very acceptable alternative. This is observed in spite of having an insufficient number of experimental parameters normally required to obtain the desired nine theoretical parameters (c and τ). The linear combination of c coefficients, which defines $S^2(\omega)$, therefore, produces a fairly stable function. In this case, pairing 500 and 600 MHz data yields better results than pairing 500 MHz (or 600 MHz) and 800 MHz data. This was surprising and should underscore the idea that acquiring relaxation at the highest magnetic field strength available may not always be necessary or desirable. However, in general, this depends on the values of the correlation times for overall tumbling and internal motions. Using the two-Lorentzian approximation (panels at the right) yields substantial error even when three spectrometer frequencies are used to calculate $S^2(\omega)$.

2. Methods and materials

The 56-residue protein GB1 was produced as a recombinant protein as described by Barchi et al. [10]. *Escherichia coli* containing the expression system for GB1 were grown on M9 minimal media containing ^{15}N -ammonium, and GB1 was uniformly isotopically enriched in ^{15}N . The protein was purified by HPLC using a linear acetonitrile/water gradient, and purity was checked by MALDI-TOF mass spectrometry and analytical HPLC on a C18 Bondclone (Phenomenex) column. For NMR measurements, freeze-dried samples were dissolved in a $\text{H}_2\text{O}/\text{D}_2\text{O}$ (95/5) mixture in 20 mM potassium phosphate. Protein concentration, determined from the dry weight of freeze-dried samples, was 10 mg/mL. The pH was adjusted to pH 5.25 by adding microliter quantities of NaOD or DCl.

With uniformly ^{15}N -enriched GB1, spin-lattice (T_1), spin-spin (T_2) relaxation times and $^{15}\text{N}\{-^1\text{H}\}$ NOEs were measured at three Larmor precession frequencies (^1H frequencies of 500, 600, and 800 MHz) on Varian Inova 500, 600, and 800 NMR spectrometers equipped with triple-resonance probes. The temperature was set at 15 °C. Temperature calibration was performed by using the chemical shifts of resonances from methanol.

^{15}N spin-lattice and spin-spin relaxation rates were measured by using the HSQCSE sequence [11], which employs pulsed field gradients for the coherence transfer pathway whereby magnetization passes from ^1H to ^{15}N and back again to ^1H for observation. The water flip-back method was used to minimize water saturation during the pulse sequence. The delay in the CPMG train was set to 0.625 ms. To attenuate cross-correlation

between dipolar and chemical-shift anisotropy terms during the relaxation period, 180° pulses of alternating phase with an interval of 5 ms were applied [12,13]. Spectra were recorded by using relaxation delays of 40, 60, 90, 160, 250, 360, and 490 ms for T_1 and 20, 40, 60, 90, 120, 180, and 240 ms for T_2 . During the relaxation delay, t_R , water magnetization affected by these ^1H 180° pulses decreases proportionally to $\exp(-t_R/T_1 \text{ water})$. Consequently, in the presence H(N)–water proton exchange, conditions will be different at the beginning of the first INEPT in the pulse sequence for experiments acquired with different values of the relaxation delay and T_1 (or T_2) will be underestimated. In order to eliminate this effect, a compensation period (CP) with the same pulse sequence as it is in the relaxation period was included prior to the recycle period at the beginning of the pulse sequence. The compensation period varies in length with the relaxation time, t_R , and is defined by $\text{CP} = t_{\text{max}} - t_R$, where t_{max} is the maximal relaxation time for a given set of experiments. By using this scheme, the same average values for the saturation of water and protein resonances have been achieved. It also allows to avoid different sample heating during the set of relaxation experiments with various relaxation delays. Recovery of magnetization of nuclei from the protein depends only on the recycle period because ^1H 180° pulses prohibit recovery of magnetization during the compensation period. For all T_1 and T_2 experiments, the recycle period was 1.7 s, and all relaxation curves followed single exponential decay.

Steady-state $\{^1\text{H}\}$ – ^{15}N NOEs were determined from three spectra recorded with proton broad band irradiation and in the absence of proton saturation with different water saturation conditions to compensate for H(N)–water proton exchange [14]. Saturation was achieved by application of 120° ^1H pulses applied every 5 ms [15] during the 3 s recycle period.

Although the length of the N–H amide bond used in ^{15}N relaxation studies is the subject of an ongoing debate [16], it was set here to 1.02 Å [17] as is usually done in such studies. All calculations were performed by using the program FRELAN, which is available at www.nmr-relaxation.com.

3. Results and discussion

To illustrate the frequency-dependent order parameter approach, ^{15}N NMR relaxation measurements were performed with the 56 residue immunoglobulin-binding domain of streptococcal protein G, GB1. Table 1 gives sequence-averaged relaxation parameters (T_1 , T_2 , and ^{15}N – $\{^1\text{H}\}$ NOE) measured at three magnetic field strengths (^1H frequencies of 500, 600, and 800 MHz) as described in [9], and complete relaxation data are given as supplemental information. $S^2(\omega)$ functions were de-

Table 1
Sequence-averaged ^{15}N NMR relaxation parameters for GB1 at 5°C at three spectrometer frequencies

Experiment	Average value
T_1 (500 MHz)	422 ± 44 ms
T_1 (600 MHz)	474 ± 45 ms
T_1 (800 MHz)	561 ± 44 ms
T_2 (500 MHz)	180 ± 19 ms
T_2 (600 MHz)	172 ± 18 ms
T_2 (800 MHz)	150 ± 15 ms
NOE (500 MHz)	-0.31 ± 0.08
NOE (600 MHz)	-0.27 ± 0.06
NOE (800 MHz)	-0.20 ± 0.05

termined for ^{15}NH backbone bonds from these ^{15}N NMR relaxation data. Fig. 3 shows calculated $S^2(\omega)$ functions for NHs of five residues in GB1: I6, T11, L12, T16, and V29. Similar appearing functions are observed for all NHs in the protein. Fitting errors are exemplified in the insert for only residue L12 for clarity. As expected from model results shown in Fig. 2, maximal error is found in the transition regions.

Three plateaus are observed in these $S^2(\omega)$ curves (Fig. 3). The first plateau occurs at high frequency where $1/\omega < 600$ ps. NMR relaxation parameters are least sensitive to motional correlation times less than about 200 ps. Therefore, all contributions to $S^2(\omega)$ from 0 to 200 ps can be considered more or less as a constant described by S_f^2 (see Fig. 1). Motional contributions over the range from 200 to 600 ps are minimal, and the $1/\omega$ transition up to $S^2(\omega) = 1.0$ cannot be determined due to a lack of experimental data in this high frequency regime. At lower frequencies where $1/\omega > 600$ ps, $S^2(\omega)$

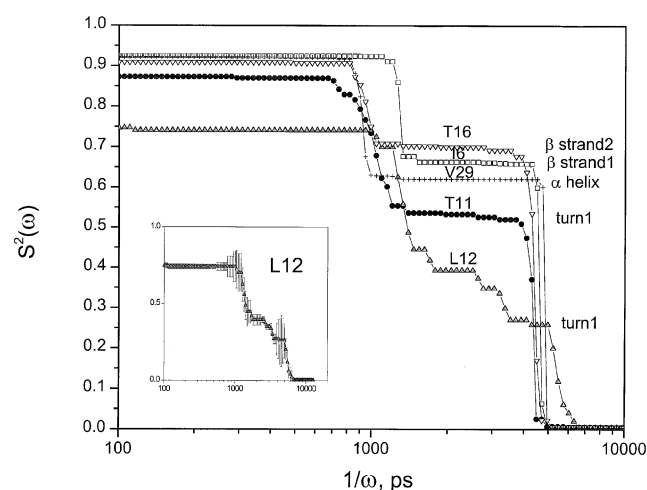


Fig. 3. $S^2(\omega)$ functions are shown for NH backbone bonds of five residues in protein GB1 (I6, T11, L12, T16, and V29). $S^2(\omega)$ was calculated using ^{15}N NMR relaxation data acquired at three frequencies (500, 600, and 800 MHz ^1H spectrometer frequencies) at 15°C . Errors for points on the $S^2(\omega)$ curve for residue L12 are shown in the insert and were determined as discussed in Section 1.

drops substantially. This is the likely range for high amplitude, internal motions, most probably related to conformational jumps. The time scale for these internal motions runs from 800 to 2000 ps. Most importantly, internal motions on this nanosecond time scale are noted for all NHs in protein GB1. This observation stands in contrast to those made in previous protein dynamics studies on GB1 [18,19], wherein only a few NHs (different in each of these studies) were reported to undergo nanosecond time scale internal motions.

The final drop in $S^2(\omega)$ to zero (Fig. 3) is related to overall tumbling, τ_o , which is equal to about 4.8 ns. τ_o values are somewhat different for individual residues due to anisotropic rotational diffusion of the molecule and to different orientations of the NH bond within the molecular frame. To demonstrate that proper parameters can be extracted using our approach, theoretical values for τ_o were calculated using averaged structural coordinates for GB1 [PDB database, access code: GB1] [20] and our program TENSOR II [4], which employs a full anisotropic rotational diffusion model based on analysis of intermolecular interactions. In Fig. 4, calculated τ_o values are plotted vs. τ_o values derived using our procedure. The linear dependence (correlation coefficient of 0.74) demonstrates the reliability of the $S^2(\omega)$ approach.

The height of the plateau between steps is essentially the order parameter. NHs of residues T11 and L12, which are part of the first turn connecting β -strands 1 and 2 in the protein, show the smallest order parameters, consistent with the general observation that residues within turns and loops often exhibit less restricted internal motions. On the other hand, NHs of residues I6, T16, and V29, which belong to the β -sheet and α -helix domains, display more restricted internal motions, i.e., larger order parameters. The width of the transition around 1 ns is primarily determined by experimental error, which depends on the value of S^2 . The largest errors are observed for NHs of more mobile residues.

For all NHs in GB1, Fig. 5 plots $S^2(\omega)$ values as columns to represent points on $S^2(\omega)$ curves taken at

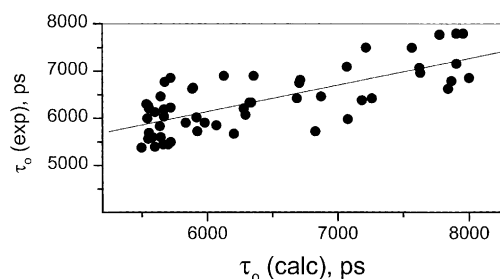


Fig. 4. Theoretical values for overall tumbling times, τ_o , are plotted vs. τ_o values determined using the new approach. Theoretical values for τ_o were calculated using averaged structural coordinates for GB1 (PDB database, access code: GB1) [19] and our program TENSOR II [4], which employs a full anisotropic rotational diffusion model.

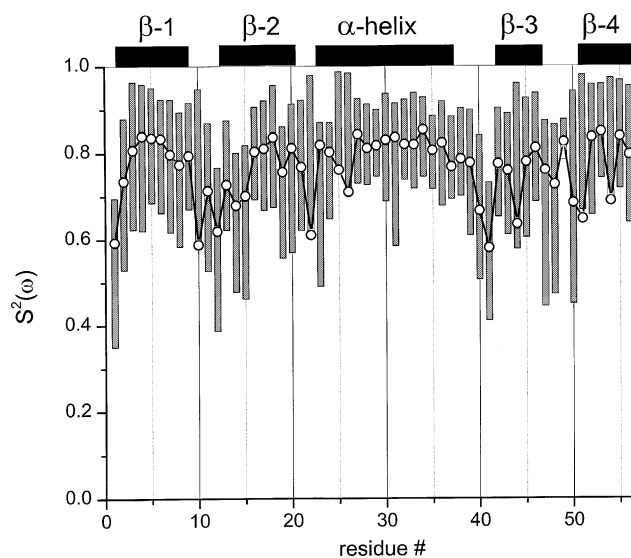


Fig. 5. Values of $S^2(\omega)$ for NH backbone bonds for all residues in protein GB1 are shown as columns to represent points on $S^2(\omega)$ curves taken at two reciprocal frequencies, $1/\omega$: 300 ps (top of columns) and 2000 ps (bottom of columns). The top end of each column is the squared order parameter for fast internal motions, S_f^2 , and the bottom end of each column represents the squared order parameter for all internal motions (the generalized order parameter, S^2). Order parameters calculated using two Lorentzians (the Lipari–Szabo method) are plotted as open circles connected by solid lines.

two reciprocal frequencies, $1/\omega$: 300 ps (top of columns) and 2000 ps (bottom of columns). The top end of each column is the squared order parameter for fast internal motions, S_f^2 , and the bottom end of each column represents the squared order parameter for all internal motions (the generalized order parameter, S^2). The lowest $S^2(\omega)$ values are observed for NHs in turns/loop and the N-terminus of the protein. NHs of residues at the middle to C-terminal part of the helix are some of the most motionally restricted. For comparison, order parameters calculated using two Lorentzians (the Lipari–Szabo method) are also plotted in Fig. 5 as open circles. These S^2 values usually lie near the middle of these $S^2(\omega)$ columns, indicating that use of the Lipari–Szabo method tends to yield overestimated generalized order parameters. This should stand as a cautionary note to investigators.

Lastly, because many researchers interested in protein dynamics do not have the luxury of being able to acquire NMR relaxation data at three spectrometer frequencies, Fig. 6 illustrates $S^2(\omega)$ curves calculated using full (three frequencies) and reduced (one or two frequencies) ^{15}N NMR relaxation data sets. Although this comparison is being shown for only one residue, E19, similar results are observed using any of the other residues in the protein. $S^2(\omega)$ curves have also been calculated using both five- and two-Lorentzian approximations. As noted earlier (Fig. 2), using the full set of relaxation data (500, 600, and 800 MHz) and the five-Lorentzian

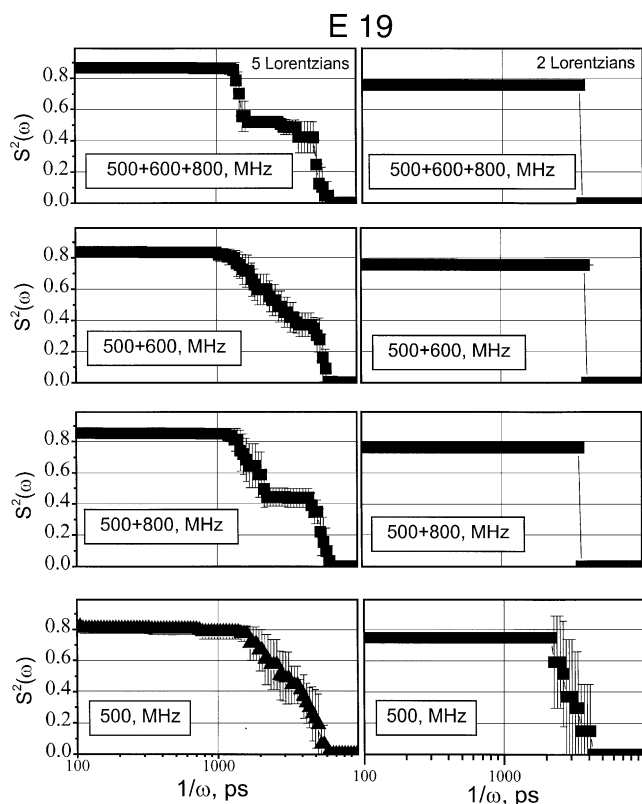


Fig. 6. An example of $S^2(\omega)$ curves calculated for E19 is shown using NMR relaxation data acquired at one, two, or three spectrometer frequencies. $S^2(\omega)$ curves have been calculated using both five- (left panels) and two- (right panels) Lorentzian approximations of the spectral density function.

approximation yields the best results. Nevertheless, use of only the 500 and 800 MHz data provides nearly the same results in this instance. Unlike the case shown in Fig. 2, the 500/600 MHz combination with these data did not work as well as the 500/800 MHz combination in the simulated data set. As was the case with these model calculations (Fig. 2), it remains clear that using only two Lorentzians to describe the spectral density function leads to significant errors in fitting NMR relaxation data.

In conclusion, the analytical approach described here allows one to visualize the frequency dependence of order parameters and more easily assess contributions to the order parameter from different motional frequencies over the picosecond to nanosecond range. This method permits the use of the maximal number of Lorentzians (correlation times) allowed by a given set of experimental data and avoids errors that arise from incorrect assumptions regarding the number of motional modes. The values of $S^2(\omega)$ for ω less than $1/\tau_0$ can be compared for proteins of various sizes and in different solvents what allow to minimize errors of S^2 calculations which come from mixing contributions of slow internal motions and overall tumbling.

Acknowledgments

This work was supported by a research grant from the National Institutes of Health (NIH, GM-58008) and benefited from use of the high field NMR facility at the University of Minnesota. We would like to thank Judy Haseman for preparing ^{15}N -enriched samples of protein GB1.

References

- [1] G. Lipari, A. Szabo, Model-free approach to the interpretation of nuclear magnetic resonance relaxation in macromolecules. I. Theory and range of validity, *J. Am. Chem. Soc.* 104 (1982) 4546–4559.
- [2] G. Lipari, A. Szabo, Model-free approach to the interpretation of nuclear magnetic resonance relaxation in macromolecules. II. Analysis of experimental results, *J. Am. Chem. Soc.* 104 (1982) 4559–4570.
- [3] V.A. Daragan, K.H. Mayo, Analysis of internally restricted correlated rotations in peptides and proteins using ^{13}C and ^{15}N NMR relaxation data, *J. Phys. Chem.* 100 (1996) 8378–8388.
- [4] V.A. Daragan, K.H. Mayo, Motional model analyses of protein and peptide dynamics using ^{13}C and ^{15}N NMR relaxation, *Prog. NMR Spectrosc.* 32 (1997) 63–105.
- [5] G.M. Clore, A. Szabo, A. Bax, L.E. Kay, P.C. Driscoll, A.M. Gronenborn, Deviations from the simple two parameter model-free approach to the interpretation of nitrogen-15 nuclear magnetic relaxation of proteins, *J. Am. Chem. Soc.* 112 (1990) 4989–4991.
- [6] M. Andrec, G.T. Montelione, R.M. Levy, Estimation of dynamic parameters from NMR relaxation data using the Lipari–Szabo model free approach and Bayesian statistical methods, *J. Magn. Reson.* 139 (1999) 408–421.
- [7] D.M. LeMaster, NMR relaxation order parameter analysis of the dynamics of protein side chains, *JACS* 121 (1999) 1726–1742.
- [8] A.M. Mandel, M. Akke, A.G. Palmer III, Backbone dynamics of *Escherichia coli* ribonuclease HI: correlations with structure and function in an active enzyme, *J. Mol. Biol.* 246 (1995) 144–163.
- [9] D. Idiyatullin, V.A. Daragan, K.H. Mayo, A new approach to visualizing spectral density functions and deriving motional correlation time distributions: application to an α -helix-forming peptide and to a well-folded protein, *J. Magn. Reson.* 152 (2001) 132–148.
- [10] J.J. Barchi, B. Grasberger, A.M. Gronenborn, G.M. Clore, G.M. Investigation, of the backbone dynamics of the IgG-binding domain of streptococcal protein G by heteronuclear two-dimensional ^1H - ^{15}N NMR spectroscopy, *Protein Sci.* 3 (1994) 15–21.
- [11] N.A. Farrow, O. Zhang, A. Szabo, D.A. Torchia, L.E. Kay, Spectral density function mapping using ^{15}N relaxation data exclusively, *J. Biomol. NMR* 6 (1995) 153–162.
- [12] L.E. Kay, L.K. Nicholson, F. Delaglio, A. Bax, D.A. Torchia, Pulse sequences for removal of the effect of cross correlation between dipolar and chemical-shift anisotropy relaxation mechanisms on the measurement of heteronuclear T_1 and T_2 values in proteins, *J. Magn. Reson.* 97 (1992) 359–375.
- [13] A.G. Palmer III, N.J. Skelton, W.J. Chazin, P.E. Wright, M. Rance, Suppression of the effect of cross-correlation between dipolar and anisotropic chemical-shift relaxation mechanisms in the measurement of spin–spin relaxation rates, *Mol. Phys.* 75 (1992) 699–711.
- [14] D. Idiyatullin, V.A. Daragan, K.H. Mayo, Improved measurement of ^{15}N - $\{^1\text{H}\}$ NOEs in the presence of H(N)–water proton chemical exchange, *J. Magn. Reson.* 153 (2001) 138–143.

- [15] J.L. Markley, W.J. Horsley, M.P. Klein, Spin-lattice relaxation measurement in slowly relaxing complex spectra, *J. Chem. Phys.* 53 (1971) 3604–3605.
- [16] D.M. Korzhnev, M. Billeter, A.S. Arseniev, V.Y. Orekhov, NMR studies of Brownian tumbling and internal motions in proteins, *Prog. NMR Spectrosc.* 38 (2001) 197–266.
- [17] L.E. Kay, D.A. Torchia, A. Bax, Backbone dynamics of proteins as studied by ^{15}N inverse detected heteronuclear NMR spectroscopy: application to Staphylococcal nuclease, *Biochemistry* 28 (1989) 8972–8979.
- [18] J.J. Barchi, B. Grasberger, A.M. Gronenborn, G.M. Clore, Investigation of the backbone dynamics of the IgG-binding domain of *Streptococcal* protein G by heteronuclear two-dimensional ^1H - ^{15}N NMR spectroscopy, *Protein Sci.* 3 (1994) 15–21.
- [19] M.J. Seewald, K. Pichumani, C. Stowell, B.V. Tibbals, L. Regan, M.J. Stone, The role of backbone conformational heat capacity in protein stability: temperature dependent dynamics of the B1 domain of *Streptococcal* protein G, *Protein Sci.* 9 (2000) 1177–1193.
- [20] A.M. Gronenborn, D.R. Filpula, N.Z. Essig, A. Achari, M. Whitlow, P.T. Wingfield, G.M. Clore, A novel, highly stable fold of the immunoglobulin binding domain of *Streptococcal* protein G, *Science* 253 (1991) 657–660.